

# Effects of field modulation on Aharonov-Bohm cages in a two-dimensional bipartite periodic lattice

Gi-Yeong Oh\*

*Department of Basic Science, Hankyong National University,  
Kyonggi-do 456-749, Korea*

We study the effects of field modulation on the energy spectrum of an electron in a two-dimensional bipartite periodic lattice subject to a magnetic field. Dependence of the energy spectrum on both the period and the strength of field modulation is discussed in detail. Our main finding is that introducing field modulation drastically changes the energy spectrum and the localization properties of the system appearing in the absence of field modulation; the degeneracies induced by a uniform magnetic field are broken and the resultant energy spectrum shows a dispersive band structure, indicating that most of Aharonov-Bohm cages become unbounded. The effects of field modulation on the superconducting transition temperature and the critical current in a wire network with the same geometry are also discussed.

PACS numbers: 73.20.Dx, 71.28.+d, 71.20.-b, 71.45.Gm

## I. INTRODUCTION

The physics of magnetically induced frustration in various two-dimensional (2D) structures including square,<sup>1–3</sup> rectangular,<sup>4,5</sup> triangular,<sup>6</sup> honeycomb,<sup>7,8</sup> aperiodic,<sup>9</sup> quasiperiodic,<sup>10,11</sup> fractal,<sup>12</sup> and even random<sup>13</sup> geometries has attracted much interest in condensed-matter physics for several decades. Recently, Vidal and co-workers<sup>14</sup> presented a new localization mechanism induced by a uniform magnetic field for noninteracting electrons in a 2D bipartite periodic hexagonal structure (the so-called  $T_3$  geometry), where the unit cell contains three sites, one sixfold coordinated (called the ‘hub’ site) and two threefold coordinated (called the ‘rim’ sites). Within the tight-binding (TB) approximation, they showed that, due to fully destructive quantum interference, the eigenstates at half a magnetic flux quantum per elementary rhombus (briefly, half a flux) are extremely localized and bounded in Aharonov-Bohm (AB) cages. Very recently, Abilio and co-workers<sup>15</sup> performed transport measurements on a superconducting wire network with the  $T_3$  geometry and confirmed the field-induced localization effect by observing a depression of the superconducting transition temperature  $T_c$  and the critical current  $J_c$  at half a flux.

Since the calculations in Ref. 14 were performed under the basic assumptions of (i) the perfectness and the infinite size of the  $T_3$  geometry and (ii) the spatial uniformity of the magnetic field, it may be very interesting to address a question of what happens under the situations beyond the two assumptions. Of course, effects beyond the assumption (i) were already discussed by the authors of Ref. 14; the randomness (such as random modulations of hopping terms and fluctuations in the tiling areas and in the transmission matrix along the edges), which is inevitable in real systems, was expected to alter or even destroy the phase matching essential for the field-induced localization effect. In addition, the authors of Ref. 15 argued that the incomplete suppression of the experimentally observed  $J_c$  at half a flux might be at-

tributed to the network’s finite size. However, effects beyond the assumption (ii) are not examined yet and remain an open question. Thus, in this paper, we would like to address the question and clarify the effects of a nonuniform magnetic field on the energy spectrum and the transport properties of the  $T_3$  geometry at rational fluxes, especially at half a flux. As a concrete and simple example, we consider a magnetic field with a periodic modulation and investigate the effect of field modulation on the stability of AB cages and on the characteristics of  $T_c$  and  $J_c$ .

The contents of this paper are organized as follows. An eigenvalue equation taking into account field modulation is derived in Sec. II. Analytic and numerical results for the effects of field modulation on the energy spectrum at rational fluxes and the localization properties of the eigenstates at half a flux are presented in Sec. III. The effects of field modulation on  $T_c$  and  $J_c$  of a superconducting wire network are also discussed in this section. Finally, Sec. IV is devoted to a summary.

## II. FIELD MODULATION AND THE EIGENVALUE EQUATION

We consider an electron in a 2D rhombus tiling under a spatially modulated magnetic field as

$$\vec{B} = [B_0 + B_{mod}(x)] \hat{z}, \quad (1)$$

where  $B_0$  ( $B_{mod}$ ) denotes the uniform (modulated) part of the applied magnetic field. Among possible types of modulated fields, we pay attention to the one-dimensional (1D) sine-modulated field as

$$B_{mod}(x) = B_1 \sin\left(\frac{2\pi x}{T_x}\right), \quad (2)$$

where  $T_x$  is the period of the modulation along the  $x$  direction. Under the Landau gauge, the vector potential is given by

$$\vec{A} = \left( 0, B_0 x - \frac{B_1 T_x}{2\pi} \cos\left(\frac{2\pi x}{T_x}\right), 0 \right). \quad (3)$$

The TB equation that describes an electron on a 2D lattice subject to a magnetic field reads

$$E\psi_i = \sum_j t_{ij} e^{i\gamma_{ij}} \psi_j, \quad (4)$$

where  $t_{ij}$  is the hopping integral between the nearest-neighbor sites  $i$  and  $j$ , and the phase factor  $\gamma_{ij}$  is given by

$$\gamma_{ij} = \frac{2\pi}{\phi_0} \int_i^j \vec{A} \cdot d\vec{l}, \quad (5)$$

$\phi_0 = hc/e$  being the magnetic flux quantum. For the sake of simplicity, we set  $t_{ij} = 1$ . The phase factor along the  $x$  direction in Fig. 1 is zero under the Landau gauge. Denoting the phase factor along the upward direction on the line 1(2, 3, 4) in Fig. 1 as  $\gamma_{1(2,3,4)}$ , and using the wave function at a hub site as  $\psi(x, y) = e^{ik_y y} \psi(x)$ , Eq. (4) can be written as

$$\begin{aligned} (E^2 - 6)\psi(x) &= \left[ e^{i(\gamma_4 + \kappa)} + e^{i(\gamma_3 + \kappa)} \right] \psi\left(x + \frac{3a}{2}\right) \\ &+ \left[ e^{2i(\gamma_3 + \kappa)} + e^{2i(\gamma_2 + \kappa)} \right] \psi(x) \\ &+ \left[ e^{i(\gamma_2 + \kappa)} + e^{i(\gamma_1 + \kappa)} \right] \psi\left(x - \frac{3a}{2}\right) + \text{H.c.}, \end{aligned} \quad (6)$$

where  $\kappa = \sqrt{3}k_y a/2$ .

Denoting  $\psi_m = \psi(x)$  at  $x = 3ma/2$ , the phase factors can be written as

$$\begin{aligned} \gamma_1 &= \frac{3\gamma}{2} \left(m - \frac{1}{2}\right) - \frac{\gamma}{2} - K \cos\left[\frac{3\pi a}{T_x} \left(m - \frac{5}{6}\right)\right], \\ \gamma_2 &= \frac{3\gamma}{2} \left(m - \frac{1}{2}\right) + \frac{\gamma}{2} - K \cos\left[\frac{3\pi a}{T_x} \left(m - \frac{1}{6}\right)\right], \\ \gamma_3 &= \frac{3\gamma}{2} \left(m + \frac{1}{2}\right) - \frac{\gamma}{2} - K \cos\left[\frac{3\pi a}{T_x} \left(m + \frac{1}{6}\right)\right], \\ \gamma_4 &= \frac{3\gamma}{2} \left(m + \frac{1}{2}\right) + \frac{\gamma}{2} - K \cos\left[\frac{3\pi a}{T_x} \left(m + \frac{5}{6}\right)\right], \end{aligned} \quad (7)$$

where

$$\gamma = 2\pi f = \frac{2\pi\phi}{\phi_0}, \quad K = \frac{\gamma\beta T_x^2}{\pi^2 a^2} \sin\left(\frac{\pi a}{2T_x}\right), \quad \beta = \frac{B_1}{B_0}, \quad (8)$$

$\phi (= \sqrt{3}B_0 a^2/2)$  being the uniform background magnetic flux through the elementary rhombus. Now let us define

$$\mu_m^\pm = \frac{\gamma_2 \pm \gamma_1}{2}, \quad \mu_{m+1}^\pm = \frac{\gamma_4 \pm \gamma_3}{2}, \quad \nu_m^\pm = \gamma_3 \pm \gamma_2, \quad (9)$$

and

$$\lambda = \frac{E^2 - 6}{4}. \quad (10)$$

Then, Eq. (6) can be reduced to a 1D equation, which is a generalized version of the eigenvalue equation derived in Ref. 14:

$$\lambda\psi_m = A_{m+1}\psi_{m+1} + C_m\psi_m + A_m\psi_{m-1}, \quad (11)$$

where

$$\begin{aligned} A_m &= \cos(\mu_m^-) \cos(\mu_m^+ + \kappa), \\ C_m &= \cos(\nu_m^-) \cos(\nu_m^+ + 2\kappa), \end{aligned} \quad (12)$$

with

$$\begin{aligned} \mu_m^- &= \frac{\gamma}{2} + K \sin\left(\frac{\pi a}{T_x}\right) \sin\left[\frac{3\pi a}{T_x} \left(m - \frac{1}{2}\right)\right], \\ \mu_m^+ &= \frac{3\gamma}{2} \left(m - \frac{1}{2}\right) - K \cos\left(\frac{\pi a}{T_x}\right) \cos\left[\frac{3\pi a}{T_x} \left(m - \frac{1}{2}\right)\right], \\ \nu_m^- &= \frac{\gamma}{2} + 2K \sin\left(\frac{\pi a}{2T_x}\right) \sin\left(\frac{3\pi m a}{T_x}\right), \\ \nu_m^+ &= 3\gamma m - 2K \cos\left(\frac{\pi a}{2T_x}\right) \cos\left(\frac{3\pi m a}{T_x}\right). \end{aligned} \quad (13)$$

A close inspection of Eqs. (11) – (13) for a reduced rational flux  $f = p/q$  with mutual primes  $p$  and  $q$  enables us to write the Bloch condition along the  $x$  direction as

$$\psi_{m+N} = e^{iN\eta} \psi_m. \quad (14)$$

Here,  $\eta = 3k_x a/2$  and  $N$  is given by

$$N = \begin{cases} \text{L.C.M.}(2T, 2q), & q \neq 3q', p \neq 2p' \\ \text{L.C.M.}(2T, q), & q \neq 3q', p = 2p' \\ \text{L.C.M.}(2T, 2q'), & q = 3q', p \neq 2p' \\ \text{L.C.M.}(2T, q'), & q = 3q', p = 2p' \end{cases} \quad (15)$$

where

$$T = \begin{cases} T_x, & T_x \neq 3T'_x \\ T'_x, & T_x = 3T'_x \end{cases} \quad (16)$$

$q'$ ,  $p'$ , and  $T'_x$  being integers. Using Eqs. (11) and (14), we obtain the characteristic matrix as

$$\begin{pmatrix} C_1 & A_2 & 0 & 0 & \cdots & A_1 e^{-iN\eta} \\ A_2 & C_2 & A_3 & 0 & \cdots & 0 \\ 0 & A_3 & C_3 & A_4 & \cdots & 0 \\ \vdots & \vdots & \vdots & \vdots & \ddots & \vdots \\ A_1 e^{iN\eta} & 0 & 0 & 0 & \cdots & C_N \end{pmatrix}. \quad (17)$$

Thus, by diagonalizing Eq. (17), we can obtain  $2N$  energy eigenvalues  $\{\pm(6 + 4\lambda_i)^{1/2}; i = 1, 2, \dots, N\}$  for a given  $\vec{k}$  and the full energy spectrum by sweeping all the  $\vec{k}$  points in the magnetic Brillouin zone (MBZ).

### III. RESULTS AND DISCUSSION

### A. $E - f$ diagram

When a periodic field modulation is introduced, a new length (i.e.,  $T_x$ ) is added into two characteristic lengths, the lattice constant  $a$  and the magnetic length  $l = (\hbar/eB_0)^{1/2}$ . Thus, a subtle interplay among them can change the energy band structure and the localization properties of the system obtained in the absence of field modulation. We plot in Fig. 2 the  $E - f$  diagrams without and with field modulation. In the calculations, we took  $T_x = 3$  and  $q = 101$  ( $1 \leq p \leq 100$ ), and swept  $(20 \times 20)$   $\vec{k}$  points in the MBZ. Comparing Fig. 2(b) with Fig. 2(a), we observe the following effects of field modulation. First, the occurrence of overlapping between neighboring subbands makes most of small gaps closed. This phenomenon of subband broadening (or gap closing) clearly appears for large values of  $\beta$  and/or  $f$ . Second, introducing field modulation lowers the symmetry of the energy spectrum. The translational symmetry [i.e.,  $E(f+1) = E(f)$ ] and the reflection invariance about  $f = 1/2$  [i.e.,  $E(f) = E(1-f)$ ] appearing in a uniform magnetic field are no longer held in the presence of field modulation. Note, however, that the energy spectrum still exhibits the symmetry with respect to  $E = 0$  and the reflection symmetry about  $f = 0$ . The former reflects the bipartite geometry of the rhombus tiling and the latter implies that there is no way for an electron to discern the direction of the magnetic field.

### B. Energy dispersion at half a flux

Before proceeding further, it may be worth noting that there are two types of localization effects in the  $T_3$  geometry. One is the topological localization appearing at  $E = 0$ , which originates from the local topology of the lattice.<sup>16</sup> Since this localization is well understood and independent of the magnetic field, we omit further discussion on this phenomenon. The other is the uniform field-induced localization appearing at  $E = \pm\sqrt{6}$  at half a flux.<sup>14</sup> We pay attention to how this kind of localization is influenced by introducing field modulation. Note also that, owing to the reflection symmetry about  $E = 0$ , we pay attention to the energy spectrum only with  $E > 0$  in the discussion below.

#### 1. Case of $T_x = 2$

In this case,  $N = 4$  and direct diagonalization of the  $(4 \times 4)$  Hamiltonian matrix yields the following energy dispersion:

$$E(k_x, k_y) = \pm\sqrt{6 \pm 4\lambda_{\pm}}, \quad (18)$$

where

$$\lambda_{\pm} = \{(A_+^2 + A_-^2 + A_0^2/2)^2 \pm [A_0^2(A_+^2 + A_-^2 + A_0^2/4)^2 + 4A_+^2 A_-^2 \sin^2(2\eta)]^{1/2}\}^{1/2}, \quad (19)$$

with

$$\begin{aligned} A_0 &= -\sin\left(\frac{4\beta}{\pi}\right) \cos(2\kappa), \\ A_{\pm} &= \pm \sin\left(\frac{2\beta}{\pi}\right) \cos\left(\kappa \mp \frac{\pi}{4}\right). \end{aligned} \quad (20)$$

A close inspection of Eq. (18) shows that the upper and lower edges of the energy dispersion with  $E > 0$  are given by

$$E_u = [6 + 4\sqrt{2D_1}]^{1/2}, \quad E_d = [6 - 4\sqrt{2D_1}]^{1/2}, \quad (21)$$

and the bandwidth is given by

$$\Delta = 4\sqrt{3} \left[ 1 - \left( 1 - \frac{8D_1}{9} \right)^{1/2} \right]^{1/2}, \quad (22)$$

where

$$D_1 = \sin^2\left(\frac{2\beta}{\pi}\right) \left[ 1 + 2\cos^2\left(\frac{2\beta}{\pi}\right) \right]. \quad (23)$$

Equation (22) clearly shows that the bandwidth varies from 0 to  $4\sqrt{3}$  with varying  $\beta$ . Note that this is a remarkable effect of field modulation; the modulated field breaks the degeneracy at  $E = \sqrt{6}$ , which appears in a uniform magnetic field and makes the energy spectrum dispersive.

#### 2. Case of $T_x = 3$

By means of a similar method for the case above, we have the energy dispersion

$$E(k_x, k_y) = \begin{cases} \pm \left\{ 6 \pm 4 [D_2 f(k_x, k_y)]^{1/2} \right\}^{1/2} \\ \pm \left\{ 6 \pm 4 [D_2 g(k_x, k_y)]^{1/2} \right\}^{1/2} \end{cases}, \quad (24)$$

where

$$\begin{aligned} f(k_x, k_y) &= \cos^2 \eta \cos^2 \kappa + \sin^2 \eta \sin^2 \kappa, \\ g(k_x, k_y) &= \sin^2 \eta \cos^2 \kappa + \cos^2 \eta \sin^2 \kappa \end{aligned} \quad (25)$$

and

$$D_2 = \sin^2\left(\frac{9\sqrt{3}\beta}{4\pi}\right). \quad (26)$$

An inspection of Eq. (24) shows that the upper and lower edges of the energy dispersion with  $E > 0$  are given by

$$E_u = [6 + 4\sqrt{2D_2}]^{1/2}, \quad E_d = [6 - 4\sqrt{2D_2}]^{1/2}, \quad (27)$$

and the bandwidth is given by the same form as Eq. (22) with replacing  $D_1$  by  $D_2$ , which varies from 0 to  $4\sqrt{2}$  with varying  $\beta$ . We plot in Fig. 3 the energy spectrum as a function of  $\beta$ , where the vertical lines are results obtained by numerically diagonalizing Eq. (17) and the boundary curves are obtained directly from Eq. (27). The inset shows the  $\beta$  dependence of the energy spectrum up to  $\beta = 6$ . The formation of a dispersive energy spectrum instead of a highly degenerate point spectrum can be clearly seen in the figure.

Another remarkable effect of field modulation can be found in the density of states (DOS). We plot in Fig. 4 the DOS for several values of  $\beta$ . The DOS for  $\beta = 0$  consists of a  $\delta$ -function peak at  $E = \sqrt{6}$ , as elucidated in Ref. 14. However, when  $\beta \neq 0$ , the DOS at  $E = \sqrt{6}$  vanishes and  $E = \sqrt{6}$  becomes an edge that connects the two subbands whose DOS's exhibit the well-known pagoda shapes with a logarithmic singularity in the middle of the subbands. The formation of a dispersive energy spectrum and the vanishing of the DOS at  $E = \sqrt{6}$  indicate that the modulated field makes most of AB cages unbounded, which in turn implies that the transport properties of the system at half a flux will exhibit quite different behaviors from those under a uniform magnetic field.

### 3. Case of $T_x \geq 4$

As an example to illustrate the fact that the energy spectrum sensitively depends not only on  $\beta$  but also  $T_x$ , we plot in Fig. 5 the energy spectrum for  $T_x = 4$  as a function of  $\beta$ . In this case,  $N = 8$  and there are eight subbands with  $E > 0$ , some of which may overlap or may have finite gaps between them depending on  $\beta$ . Figure 5 shows that the number of distinguishable subbands runs from 1 to 6 with increasing  $\beta$  up to 1. We found that the occurrence of subband splitting (or gap opening) is a generic feature of the energy spectrum at half a flux for  $T_x \geq 4$ . We also found that the subband splitting occurs more easily when  $T_x \neq 3T'_x$  than when  $T_x = 3T'_x$ .

The  $T_x$  dependence of the DOS also exhibits an interesting feature. For illustrative purposes, we plot in Fig. 6 the DOS for  $T_x = 4$  for several values of  $\beta$ . It can be seen that  $E = \sqrt{6}$  locates near an edge of a subband for small values of  $\beta$ , while it locates in a subband for large values of  $\beta$ . Note, however, that even in the latter case the DOS at  $E = \sqrt{6}$  is still negligibly small compared with the integrated DOS and will have a very little effect on the transport properties of the system, if any.

### C. Energy dispersion at generic rational fluxes

The  $\beta$  dependence of the energy spectra for generic rationals  $f$  exhibits a behavior similar to the case of  $f = 1/2$ ; the phenomena of subband broadening and gap opening are generic features under the modulated field.

We show an example in Fig. 7, where the energy spectrum with  $E > 0$  is plotted for  $f = 2/3$  and  $T_x = 4$ . When  $\beta = 0$ , the energy spectrum consists of two subbands that touch each other at  $E = 0$ , resulting in a gapless single-band structure.<sup>14</sup> However, when the field modulation is turned on, a gap opens between the two subbands. Besides, with increasing  $\beta$ , there occurs further splitting of each subband into several sub-subbands as well as the gap closing and reopening.

### D. Effect of $\beta$ on $T_c$ in a wire network

Now we are in position to discuss the effects of field modulation on  $T_c$  and  $J_c$  in a wire network. In the case of the  $T_3$  geometry,  $T_c(f)$  is directly related to the edge eigenvalue of Eq. (11) by<sup>2,15</sup>

$$1 - \frac{T_c(f)}{T_c(0)} = C \left[ \arccos \left( \frac{E_e(f)}{\sqrt{18}} \right) \right]^2, \quad (28)$$

where  $C$  is a constant that is proportional to the square of the superconducting coherence length at zero temperature and  $E_e(f)$  is the edge eigenvalue at a rational flux  $f$ . For simplicity, we set  $C = 1$ .

We plot in Fig. 8 the phase boundaries for a system with  $T_x = 3$ . In the calculations, we took  $q = 101$  ( $1 \leq p \leq 100$ ). It can be clearly seen that the phase boundary for  $\beta = 0$  is symmetric about  $f = 1/2$  and distinct downward cusps occur at low order rationals  $f = 1/3, 2/3, 1/6, 5/6, 2/9$ , and  $7/9$ . Besides, an upward cusp exists at  $f = 1/2$ , which reflects the field-induced localization properties of the eigenstates at half a flux, as demonstrated in Ref. 15. However, when the field modulation is introduced, the phase boundary exhibits several distinctive features from the case of  $\beta = 0$  as follows. First, the phase boundary becomes asymmetric with respect to  $f = 1/2$ , which reflects the breaking of the reflection invariance of the energy spectrum about  $f = 1/2$ . Second, the phase boundary for  $f \geq 1/3$  severely changes in a nontrivial way even for small values of  $\beta$ , while the boundary for  $f \leq 1/3$  is less influenced even by large values of  $\beta$ . To put it concretely, of the cusps at strong commensurate fields exhibited in the absence of field modulation, the cusps at  $f = 1/3$  and  $1/6$  are still clearly visible, while the cusp at  $f = 5/6$  becomes invisible by introducing field modulation. Meanwhile, the cusp at  $f = 2/3$  is visible (invisible) at  $\beta = 0, 0.6$  ( $\beta = 0.3$ ). Third, with increasing  $\beta$ , the  $T_c(f)$  depression up to  $f \leq 4/5$  decreases independently of  $T_x$ . The  $\beta$  dependence of the  $T_c$  depression at  $f = 1/2$  is shown in Fig. 9, where a monotonic decrease of  $1 - T_c(f)/T_c(0)$  is clearly seen. Meanwhile, the amount of the  $T_c$  depression for  $f \geq 4/5$  is inconsistent with the modulation strength. Fourth, the cusp at  $f = 1/2$  moves downward by introducing a field modulation, which is the most remarkable effect of field modulation on  $T_c$ . This phenomenon indicates that the localization properties of the system at

$f = 1/2$  becomes similar to those at other rational fluxes (such as  $f = 1/3, 1/2, 1/6, 5/6$ ) in which the eigenstates exhibit an extended nature. Fifth, the value of  $f$  where the maximal  $T_c$  depression is achieved lowers as  $\beta$  increases.

Now, let us briefly discuss the effect of field modulation on the critical current  $J_c(f)$ , which is closely related to the band curvature,  $\partial^2 E_e(f)/\partial k^2$ , near the band edge. When  $\beta = 0$ , due to the absence of dispersive states,  $J_c(f = 1/2)$  vanishes completely, as discussed in Ref. 15. However, when  $\beta \neq 0$ , the formation of a dispersive band structure makes  $\partial^2 E_e(f)/\partial k^2 \neq 0$ , and hence  $J_c(f = 1/2)$  will have a finite value, which is another remarkable effect of field modulation.

#### IV. SUMMARY

We have studied the effects of field modulation on the energy spectrum of an electron in a 2D bipartite periodic lattice subject to a magnetic field and on the superconducting transition temperature in a wire network with the same geometry. We have shown that the energy spectrum sensitively depends on both the period and the strength of field modulation. Our main finding is that the field-induced localization properties of the lattice at half a flux are drastically changed by introducing field modulation; the modulated field breaks the degeneracy induced by a uniform magnetic field to make the energy spectrum dispersive, where the number of distinguishable subbands sensitively depends on both the period and the strength of field modulation. The formation of a dispersive energy spectrum in turn has been shown to crucially influence the superconducting transition temperature and the critical current of the wire network. Before concluding this paper, we would like to make a few remarks. First, though we treated only the  $T_3$  geometry in this paper, we expect that the field-induced localization properties of the  $T_4$  geometry<sup>14</sup> will undergo similar effects of field modulation. Second, for the sake of simplicity in the calculation, we dealt with a simple case where the period of field modulation is commensurate with the lattice period. The energy spectrum may exhibit more complicated band structures when the two length scales are incommensurate with each other. Finally, note that the magnetic flux treated in this paper is neither uniform nor random but periodic. Thus, the effects of a random magnetic flux is still an open question, and it would be interesting to study whether or not AB cages remain bounded and/or how the localization properties of the system are influenced by introducing a random flux. Our naive expectation is that switching on a random flux at  $f = 1/2$  will induce an energy band of localized states.

#### ACKNOWLEDGMENTS

This work was financially supported by Hankyong National University, Korea, through the program year of 1999.

- 
- \* Electronic address: ogy@hnu.hankyong.ac.kr
- [1] R. Peierls, *Z. Phys.* **80**, 763 (1933); P. G. Harper, *Proc. Phys. Soc. London Sect. A* **68**, 874 (1955); W. Kohn, *Phys. Rev.* **115**, 1460 (1959); M. Ya Azbel, *Zh. Eksp. Teor. Fiz.* **46**, 929 (1964) [*Sov. Phys. JETP* **19**, 634 (1964)]; D. R. Hofstadter, *Phys. Rev. B* **14**, 2239 (1976); G. H. Wannier, *Phys. Status Solidi B* **88**, 757 (1978).
  - [2] P. G. de Gennes, *C. R. Seances Acad. Sci., Ser. B* **292**, 9 (1981); **292** 279 (1981); S. Alexander, *Phys. Rev. B* **27**, 1541 (1983); R. Rammal, T. C. Lubensky, and G. Toulouse, *ibid.* **27**, 2820 (1983); S. N. Sun and J. P. Ralston, *ibid.* **43**, 5375 (1991).
  - [3] B. Pannetier, J. Chaussy, R. Rammal, and J. C. Villegier, *Phys. Rev. Lett.* **53**, 1845 (1984); O. Buisson, M. Giroud, and B. Pannetier, *Europhys. Lett.* **12**, 727 (1990); M. A. Itzler, R. Bojko, and P. M. Chaikin, *ibid.* **20**, 639 (1992).
  - [4] A. Borelli, J. Bellissard, and F. Claro, *Phys. Rev. Lett.* **83**, 5082 (1999).
  - [5] C. R. Hu, *Phys. Rev. B* **35**, 5294 (1987); C. R. Hu and R. L. Chen, *ibid.* **37**, 7907 (1988).
  - [6] D. Langbein, *Phys. Rev.* **180**, 633 (1969); F. H. Claro and G. H. Wannier, *Phys. Rev. B* **19**, 6068 (1979); D. J. Thouless, *ibid.* **28**, 4272 (1983); Y. Hasegawa, Y. Hasegawa, M. Kohmoto, and G. Montambaux, *ibid.* **41**, 9174 (1990); G. Y. Oh, *J. Phys.: Condens. Matter* **12**, 1539 (2000).
  - [7] T. Horiguchi, *J. Math. Phys.* **13**, 1411 (1972); R. Rammal, *J. Phys. (France)* **46**, 1345 (1985); V. A. Geyler and I. Yu Popov, *Z. Phys. B* **98**, 473 (1995).
  - [8] B. Pannetier, J. Chaussy, and R. Rammal, *J. Phys. (France)* **44**, L853 (1983).
  - [9] P. Santhanam, C. C. Chi, and W. W. Molzen, *Phys. Rev. B* **37**, 2360 (1988); F. Nori and Q. Niu, *ibid.* **37**, 2364 (1988).
  - [10] M. Arai, T. Tokihiro, and T. Fujiwara, *J. Phys. Soc. Jpn.* **56**, 1642 (1987); T. Hatakeyama and H. Kamimura, *ibid.* **58**, 260 (1989); Q. Niu and F. Nori, *Phys. Rev. B* **39**, 2134 (1989); M. A. Itzler, R. Bojko, and P. M. Chaikin, *ibid.* **47**, 14165 (1993); H. Schwabe, G. Kasner, and H. Böttger, *ibid.* **56**, 8026 (1997).
  - [11] A. Behrooz, M. J. Burns, H. Deckman, D. Levine, B. Whitehead, and P. M. Chaikin, *Phys. Rev. Lett.* **57**, 368 (1986).
  - [12] R. Rammal and G. Toulouse, *Phys. Rev. Lett.* **49**, 1194 (1982); J. R. Banavar, L. Kadanoff, and A. M. M. Pruisken, *Phys. Rev. B* **31**, 1388 (1985); X. R. Wang, *ibid.* **53**, 12035 (1996); A. Chakrabarti and B. Bhattacharyya, *ibid.* **56**, 13786 (1997); Y. Liu, Z. Hou, P. M. Hui, and W. Sritrakool, *ibid.* **60**, 13444 (1999).

- [13] R. G. Steinmann and B. Pannetier, *Europhys. Lett.* **5**, 559 (1988).
- [14] J. Vidal, R. Mosseri, and B. Douçot, *Phys. Rev. Lett.* **81**, 5888 (1998).
- [15] C. C. Abilio, R. Butaud, Th. Fournier, B. Panneiter, J. Vidal, S. Tedesco, and B. Dalzotto, *Phys. Rev. Lett.* **83**, 5102 (1999).
- [16] B. Sutherland, *Phys. Rev. B* **34**, 5208 (1986).

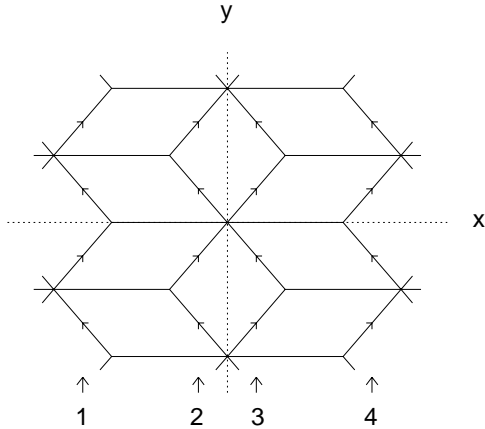


FIG. 1. A portion of the 2D bipartite periodic tiling.

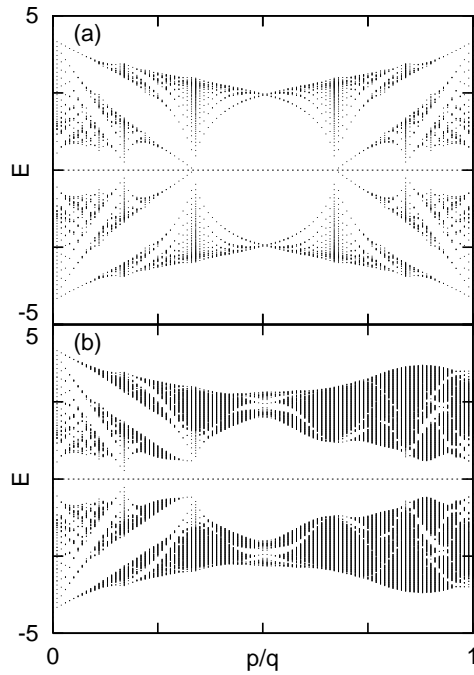


FIG. 2. Energy spectrum as a function of  $f$  for  $T_x = 3$ . (a)  $\beta = 0.0$ , (b)  $\beta = 0.3$ .

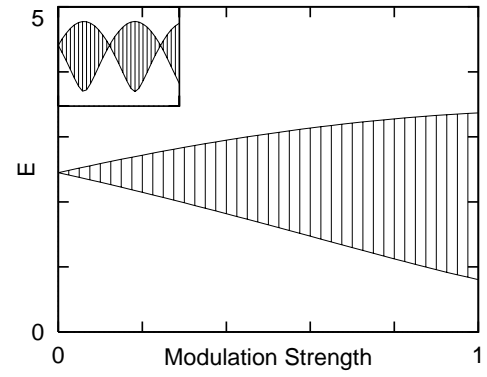


FIG. 3. Energy spectrum as a function of  $\beta$  for  $f = 1/2$  and  $T_x = 3$ .

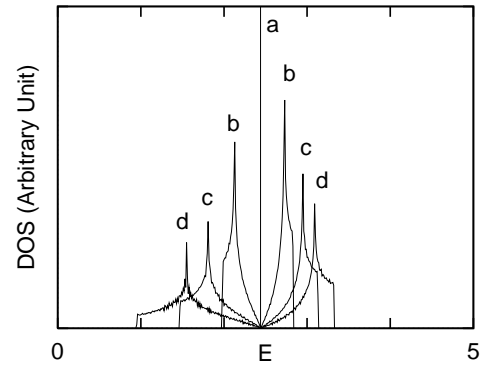


FIG. 4. Density of states for  $f = 1/2$  and  $T_x = 3$ . (a)  $\beta = 0.0$ , (b)  $\beta = 0.3$ , (c)  $\beta = 0.6$ , (d)  $\beta = 0.9$ .

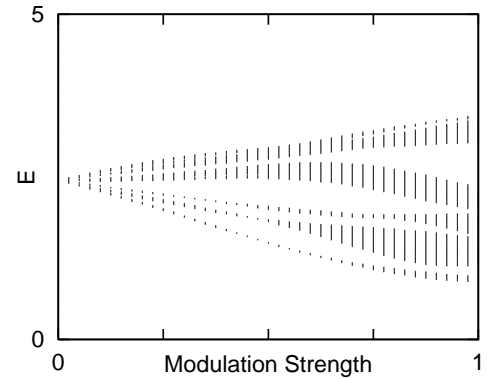


FIG. 5. Energy spectrum as a function of  $\beta$  for  $f = 1/2$  and  $T_x = 4$ .

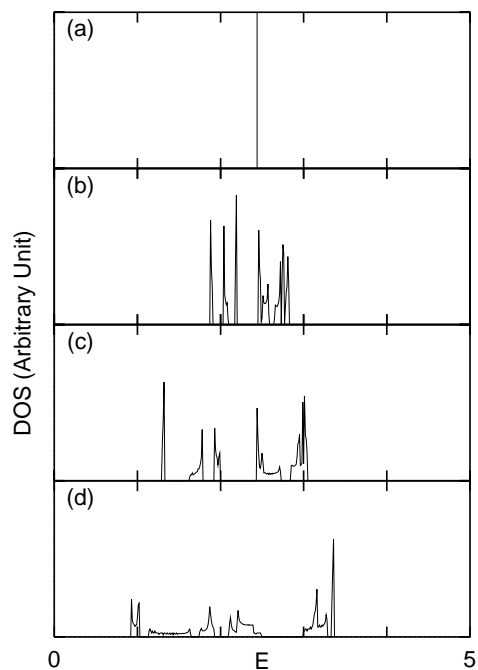


FIG. 6. Density of states for  $f = 1/2$  and  $T_x = 4$ . (a)  $\beta = 0.0$ , (b)  $\beta = 0.3$ , (c)  $\beta = 0.6$ , (d)  $\beta = 0.9$ .

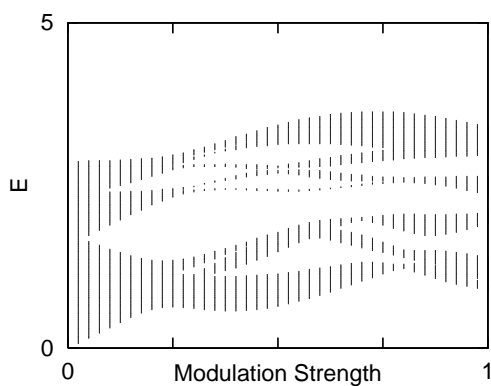


FIG. 7. Energy spectrum as a function of  $\beta$  for  $f = 2/3$  and  $T_x = 4$ .

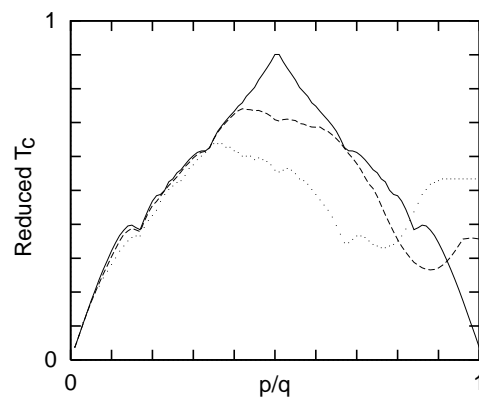


FIG. 8.  $1 - T_c(f)/T_c(0)$  as a function of  $f$  for  $T_x = 3$ . Continuous line:  $\beta = 0$ , dashed line:  $\beta = 0.3$ , dotted line:  $\beta = 0.6$ .

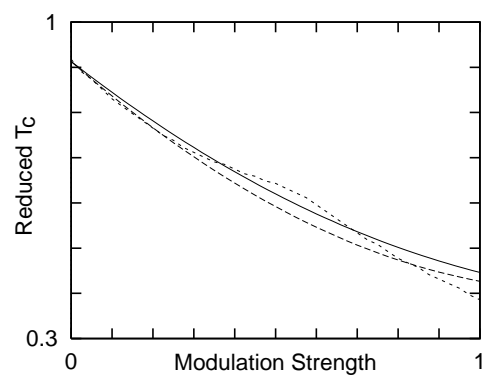


FIG. 9.  $1 - T_c(f)/T_c(0)$  as a function of  $\beta$  for  $f = 1/2$ . Continuous line:  $T_x = 2$ , long-dashed line:  $T_x = 3$ , short-dashed line:  $T_x = 4$ .